Preparation of Polypropylene/Carbon Nanotube Composite Powder with a Solid-State Mechanochemical Pulverization Process

Hesheng Xia,[1] Qi Wang,[1] Kanshe Li,[1] Guo-Hua Hu[2]

[1]*State Key Laboratory of Polymer Materials Engineering, Polymer Research Institute, Sichuan University, Chengdu 610065, China*
[2]*Laboratory of Chemical Engineering Sciences, CNRS-ENSIC-INPL, 1 Rue Grandville, BP 451, 54001, Nancy Cedex, France*

Received 23 September 2003; accepted 18 December 2003
DOI 10.1002/app.20435
Published online in Wiley InterScience (www.interscience.wiley.com).

ABSTRACT: A solid-state mechanochemical pulverization process, that is, pan milling, was used to prepare a polypropylene (PP)/carbon nanotube (CNT) composite powder. The composite powder was then melt-mixed with a twin-roll masticator to obtain a PP/CNT composite. The morphology of the PP/CNT powder and the PP/CNT composite was investigated. The crystallization and mechanical properties of the latter were also studied. After 20 milling cycles (ca. 60 min), the average diameter of PP/3 wt % CNT composite powder particles was a few micrometers. The length of the CNTs was reduced from a few micrometers to 0.4–0.5 μm. The CNTs became straighter and more uniform in length. The effects of incorporating the CNTs into PP were as follows: (1) the crystallization rate and temperature of PP increased, (2) a strong *b*-plane orientation of PP was induced, and (3) the Young's modulus and yield strength of PP increased. Interfacial adhesion between PP and the CNTs was improved by the mechanical action of the solid-state pulverization process used, which favored the dispersion of the CNTs into PP. © 2004 Wiley Periodicals, Inc. J Appl Polym Sci 93: 378–386, 2004

Key words: nanocomposites; poly(propylene) (PP); shear

INTRODUCTION

Because carbon nanotubes (CNTs) can be produced on a large scale, CNT/polymer composites have attracted much attention.[1–6] CNTs are ideal reinforcing fibers for polymers because they have high aspect ratios, high mechanical strength, and high electrical and thermal conductivity.[7,8] Also, in comparison with conventional carbon or glass fibers, CNT-filled polymer composites are easier to mold, and articles thereof have much better surface appearance, even if they are highly loaded with CNTs. They retain most of the properties of the polymer matrix (elasticity, strength, and modulus) and have the additional functionality of exceptionally high electrical and thermal conductivity. CNT/polymer composites open up opportunities for new multifunctional materials with broad applications. However, the preparation of such materials faces challenges, such as ensuring the uniform dispersion of CNTs in polymer matrices without agglomerates and entanglements and adequate interfacial adhesion between the CNTs and polymers. One way of solving these problems is to modify the surface properties of CNTs by chemical modification and functionalization, surfactant treatment, and polymer wrapping.[9–17] This usually involves complicated organic treatment processes.

Mechanochemistry, including mechanoactivation, mechanoinitiation, and mechanosynthesis, is an alternative. It deals with stress-induced chemical reactions and structural changes of materials. Mechanochemical processes, such as high-energy ball milling, vibromilling, pan milling, and jet milling, can be used to prepare ultrafine metal, inorganic oxide, and polymer powders on a large scale and to activate their surfaces.[18–21] In this work, a solid-state mechanochemical process, that is, pan milling, was used to prepare CNT/polymer composite powders. The powders were melt-mixed with a twin-roll masticator to obtain composite materials. The pan-milling equipment was designed in our laboratory for solid-state mechanochemical reactions of polymers.[22] A theoretical analysis has demonstrated that this equipment has strong pulverizing and mixing effects on polymeric materials because of an ingenious design inspired by a traditional Chinese stone mill. Acting as three-dimensional

Correspondence to: Q. Wang (qiwang@scu.edu.cn).
Contract grant sponsor: Special Funds for Major State Basic Research Projects of China; contract grant number: G1999064809.
Contract grant sponsor: National Natural Science Foundation of China; contract grant number: 200340061.
Contract grant sponsor: China–France Advanced Research Program; contract grant number: PRAMX00-08.

scissors, our pan mill has the ability to generate a strong squeezing force in the normal direction and a strong shearing force in both the radial and tangential directions. As such, both particle size reduction and chain scission of polymers may occur during the pan-milling process. Commodity polymers such as polypropylene (PP) and engineering polymers such as polyamide 6 can be effectively pulverized at room temperature with our pan mill.[21] Vinyl monomers such as maleic anhydride and hydroxymethyl acrylamide have been grafted onto PP in the solid state with success.[23] In this work, that mill pan was used to prepare the CNT/PP composite powder, which could have different applications. For example, it could be directly molded into conductive or antistatic articles. It could also be thermally sprayed to form a nanocomposite coating. It could be used as a master batch that could subsequently be diluted in other polymers or as an additive to modify the mechanical, thermal, and electrical properties of polymer materials. The CNT/PP composite powder was then melt-mixed to obtain the corresponding composite material. The morphology and crystal structure of the composite powder and the crystallization behavior and mechanical properties of the composite material were studied.

EXPERIMENTAL

Materials

Multiwalled carbon nanotubes (MWCNTs) were provided by the Chengdu Institute of Organic Chemistry of the Chinese Academy of Sciences (Chengdu, China). MWCNTs were synthesized through the dissociation of methane at a high temperature of 700°C with a NiO/La_2O_3 catalyst. The outer and inner diameters of the MWCNTs were 20–30 and 5–10 nm, respectively. They were washed with concentrated hydrochloride acid for the removal of the catalyst and its carrier and then purified with concentrated HNO_3 for the removal of amorphous carbon particles. PP was supplied by Beijing Yanshan Petro-Chemical Group (Beijing, China). It was in the form of pellets 3–4 mm in diameter. Its melt-flow index and density were 0.3 g/10 min and 0.9013 g/cm^3, respectively. Xylene was purchased from the Chemical Reagent Factory (Chengdu, China).

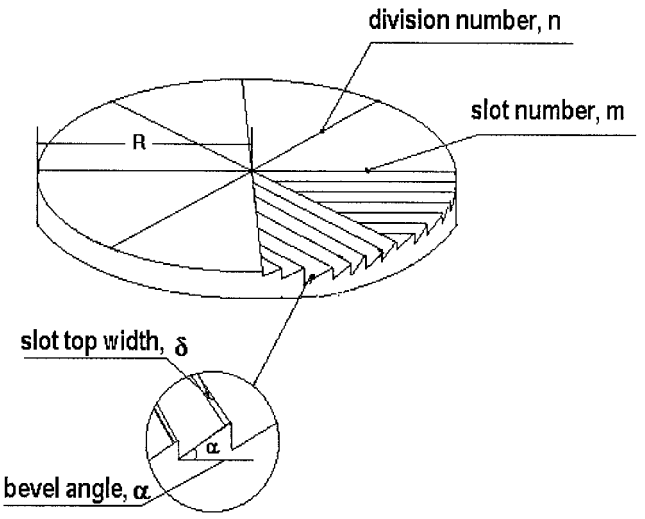

Figure 1 Schematic diagram of the structure of the inlaid mill pan in the designed pan-milling equipment.

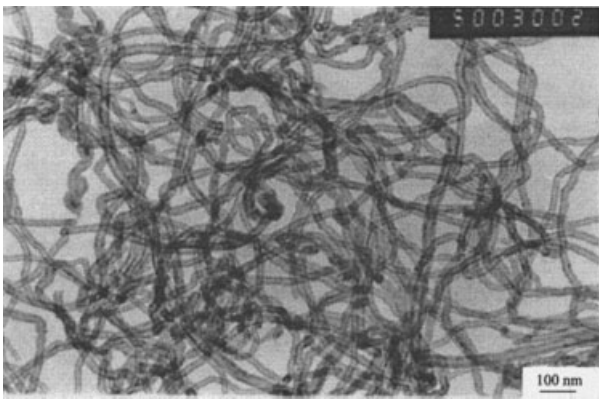

Figure 2 Transmission electron microscopy image of raw MWCNTs.

Preparation of the PP/CNT composite powder

The PP/CNT composite powder was prepared in a pan mill. It was designed in our laboratory and described in a previous article.[22] Figure 1 is a schematic drawing of its design. For a typical milling process, 200 g of PP and 1–6 g of CNTs were fed into the pan mill through a hopper located in the middle of the pan mill. The rotation speed of the pan mill was fixed at 30 rpm. Milled particles were discharged from the brim of the pan. They were collected for the next milling cycle. The process was conducted at room temperature, and the heat generated by milling was removed with cooling water.

Preparation of the PP/CNT composite

The pan-milled PP/CNT composite powder was melt-mixed for 15 min with a twin-roll masticator at 160°C. The composite material lump thus obtained was then molded into sheets (117 mm × 118 mm × 4 mm and 100 mm × 100 mm × 1.2 mm). As a control experiment, the PP and CNTs without pan milling were also melt-mixed for 15 min in the twin-roll masticator and then molded into sheets of the aforementioned dimensions.

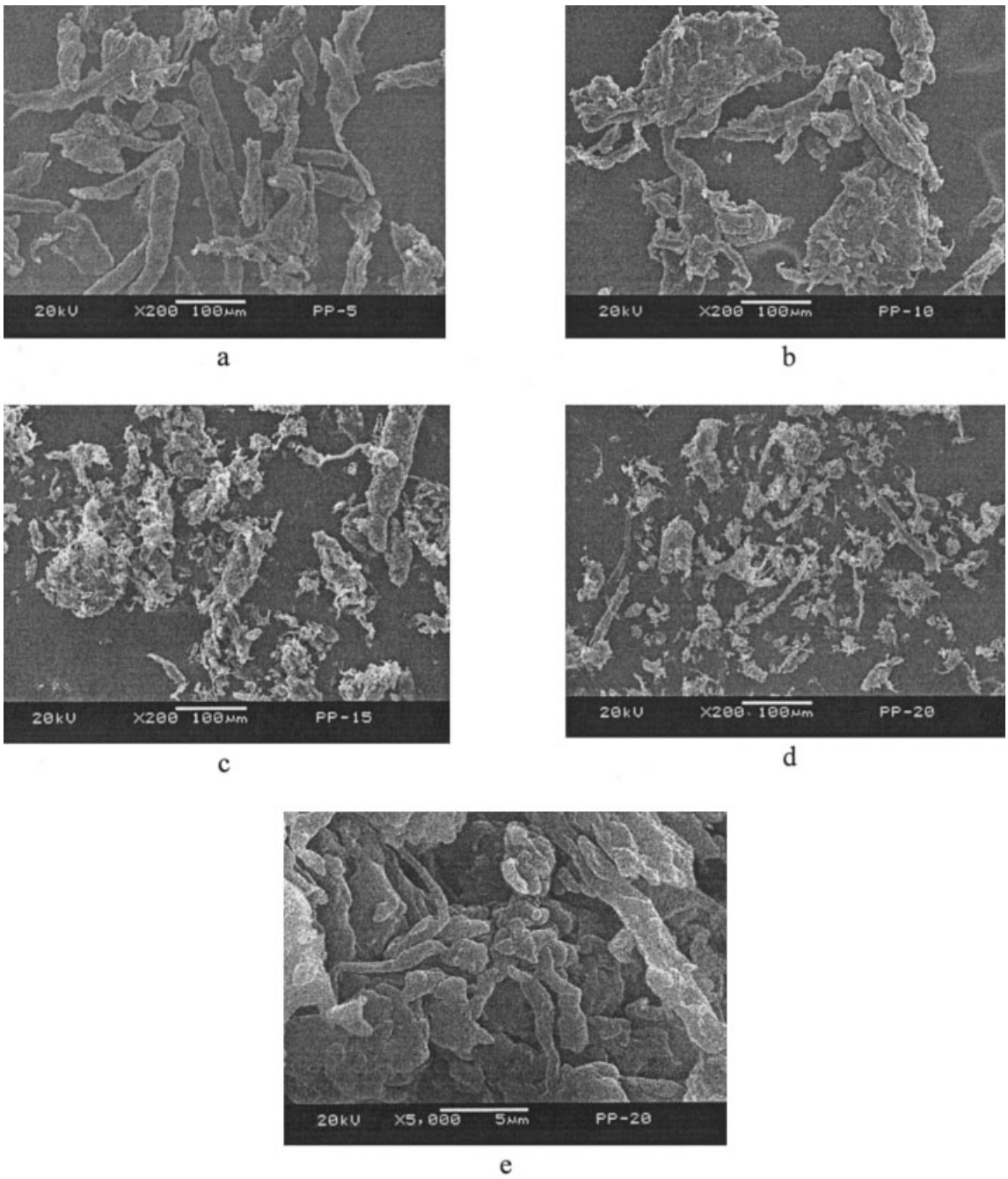

Figure 3 SEM images of PP/CNT composite powders after comilling: (a) 5, (b) 10, (c) 15, and (d,e) 20 times.

Characterization

Fourier transform infrared (FTIR) spectra of the composites were recorded on a Nicolet 560 FTIR spectrometer (USA). They were collected from 4000 to 400 cm^{-1} at a resolution of 4 cm^{-1} over 20 scans. The particle size and morphology were characterized with scanning electron microscopy (SEM; X-650, Hitachi, Japan). A surface area and porosity analyzer (2010, ASAP, USA) was used to measure the Brunauer–Emmett–Teller (BET) specific surface area of the PP/CNT composite powder (with N_2 as an analysis adsorptive and a 77.35 K analysis bath). The tensile properties were measured according to ASTM D 638 with a material tester (4302, Instron, UK) at a crosshead speed of 100 mm/min. The phase morphology was characterized with SEM (X-650, Hitachi). Specimens were cryogenically fractured in liquid nitrogen. The fractured surfaces were gold-sputtered before observation. The composite powder and molded sheets were characterized by wide-angle X-ray diffraction (XRD) with a Philips X'Pert X-ray diffractometer (The Netherlands) fitted with a goniometer detection device (40-kV an-

ode and 35-mA filament current). Nickel-filtered Cu Kα radiation with a wavelength of 0.1542 nm was directed at the samples in the transverse direction. The scanning speed of the goniometer was 0.133°/s with a step size of 0.02°. It diffracted X-rays in the 2θ range of 5–45°. The recorded XRD profiles, including the crystalline peak and amorphous halo, were fitted with Philips Analytical X-Ray Profit 1.0 software. The background profile and the aforementioned fitting parameter were first set, and then the fitting was started. After the fitting was optimized, the parameters, including the Bragg 2θ value of the peak, the intensity of the peak, the full width at half-maximum, and the area, were given. The crystallinity (XL) was obtained from the ratio of the area of the crystalline peak to the total area under the diffraction curve.[24] A Netzsch DSC 204 differential scanning calorimeter (Germany) was used to determine the melting temperature, crystallization temperature, and enthalpy of fusion of the specimens, which were analyzed by XRD. The samples (5–10 mg) were heated to 220°C at a rate of 10°C/min to remove any thermal history before they were cooled down to 30°C at the same rate. The flow rate of nitrogen was 50 mL/min. XL was measured from the area of the heating endotherm or cooling exotherm. The enthalpy of fusion for 100% crystalline PP was taken to be 138 J/g.[25,26] The temperature corresponding to the peak of the crystallization exotherm was taken as the crystallization temperature.

RESULTS AND DISCUSSION

PP/CNT composite powder

Figure 2 shows the morphology of the raw CNTs. Their diameter and length were 20–40 nm and 1–10 μm, respectively. Figure 3 shows the morphology of PP/3% CNT composite powder obtained after 5, 10, 15, and 20 milling cycles. The composite powder decreased in size with more milling cycles, and the particles became more uniform. After 20 milling cycles (ca. 60 min), the average particle size was reduced to a few micrometers. Accordingly, the BET surface area increased to 4.29 m^2/g. After the milling of the PP and CNTs, the latter were incorporated in the form. Therefore, it was not possible to measure the size of the CNTs in the composite powder. To do so, the PP in the composite powder was removed by Soxhlet extraction with xylene as the solvent. Figure 4 shows the morphology of the CNTs obtained from the composite powder after 120 h of Soxhlet extraction. After milling, the length of the CNTs was much reduced (from a few micrometers to 0.4–0.5 μm), and their diameter apparently increased greatly. Moreover, the CNTs became straighter and more uniform in size. The diameter increase was probably related to the existence of a PP layer surrounding the CNTs, which was not removed after 120 h of Soxhlet extraction. This implies that that the PP layer was strongly bound to the CNT walls. The design of the pan mill used in this work was unique. It was like three-dimensional scissors capable of generating strong shearing, squeezing, and friction when two pans were under rotation. As such, during pan milling, the CNTs were cut off, preferably at mechanically weak locations such as curvatures and side-wall defects. Short CNTs may be interesting. Chen et al.[27] cut CNTs in concentrated HNO_3 and H_2SO_4 under high-intensity ultrasound. Mechanical processes such as ball milling were used to make tailored CNTs.[28,29] The results of this work show that pan milling can also be an efficient process for cutting CNTs. Mechanical cutting reduces the aspect ratio of CNTs and, therefore, their entanglements. Moreover, it reduces the number of defects and curvatures. We expected the reinforcing performance of short CNTs with fewer defects, curvatures, and entanglements to be higher than that of long CNTs with more defects, curvatures, and entanglements. A model study showed that the reinforcing efficiency of short nanotubes with an aspect ratio of about 30 was similar to that of long ones.[30] The FTIR spectra of the CNTs used, the PP/CNT composite powder, and the CNTs obtained from the PP/CNT composite powder after 120 h of Soxhlet extraction in xylene are shown in Figure 5. The spectrum of the CNTs obtained from the composite powder after extraction had some of the characteristic peaks of PP at 2922, 2853, 1458, and 1377 cm^{-1}. This further suggests that after pan milling, some PP chains were strongly bound to the walls of the CNTs. Under the strong shearing, squeezing, and frictional actions of the pan mill, macroradicals were likely formed on PP chains, which could then chemically interact with the surfaces of the CNTs, which could also be modified during pan milling. Mechanically induced chemical reactions with polymers in a pan mill are now well known. For example, maleic

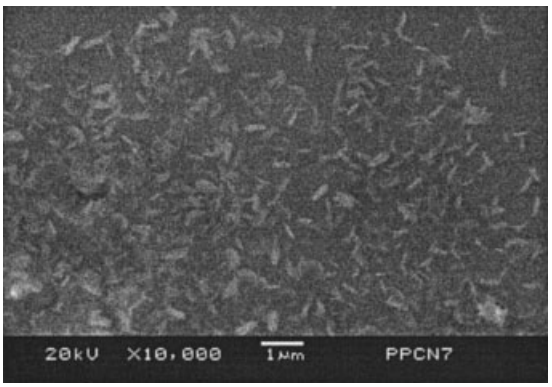

Figure 4 SEM image of shortened CNTs by pan milling (PP/3% CNT composite powder after 120 h of Soxhlet extraction with boiling xylene).

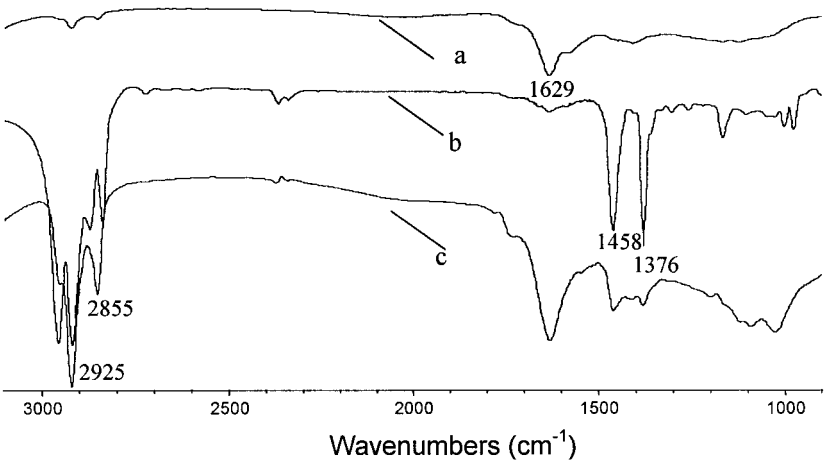

Figure 5 FTIR spectra of (a) CNTs, (b) PP/3% CNT composite powder, and (c) PP/3% CNT composite powder after 120 h of Soxhlet extraction with boiling xylene.

anhydride and hydroxymethyl acrylamide have been grafted onto polymers with success.[23]

Effects of pan milling on the crystal structure of PP

Figure 6 shows the XRD diagrams of raw PP, the PP powder obtained after the pan milling of the raw PP, a PP/CNT composite powder, and raw CNT. PP can have three crystal structures: α, β, and γ. The characteristic diffraction peaks of α (monoclinic) crystal planes (110, 040, 130, 111, and 041) appeared for all the PP samples, and this suggested that the pan-milling process did not change the crystal form. The XL values of the raw PP, PP powder, PP/1% CNT composite powder, and PP/3% CNT composite powder were 56.8, 39.4, 36.6, and 37.6%, respectively. Moreover, the diffraction peak became wider, and this indicated that the crystal size decreased. Some *d*-spacing of the crystal plane shifted, and this suggested that crystallites were deformed during pan milling. Figure 7 shows the differential scanning calorimetry (DSC) heating thermograms of the raw PP, PP powder, and PP/CNT composite powders. The XL values of PP calculated from the enthalpy of fusion were 47.3, 39.5, 38.4, and 41.5% for the raw PP, PP powder, PP/1% CNT composite powder, and PP/3% CNT composite powder, respectively. After the pan milling, the XL values of PP decreased, and this was in agreement with the results obtained from XRD. The melting peak temperature of the PP powder was approximately 144.2°C. Upon the

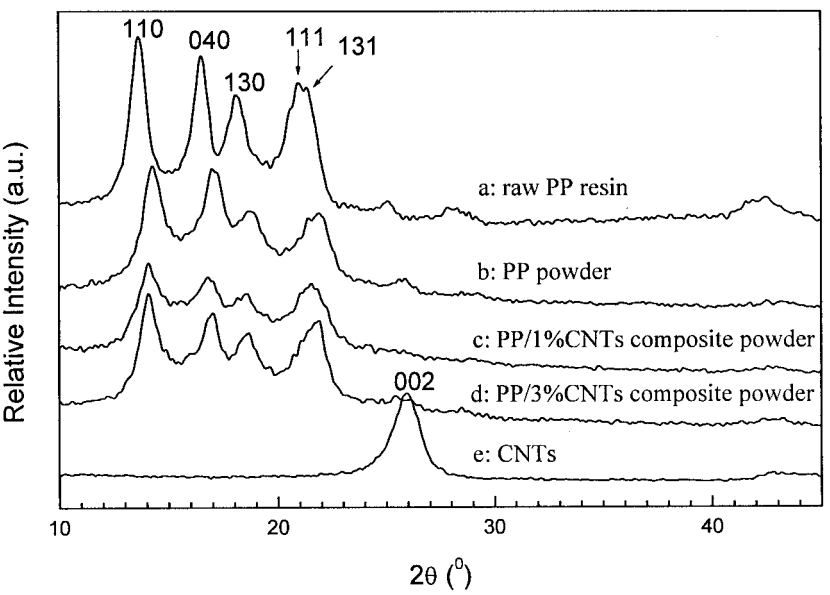

Figure 6 XRD profiles of PP resin, CNT, and PP/CNT composite powders.

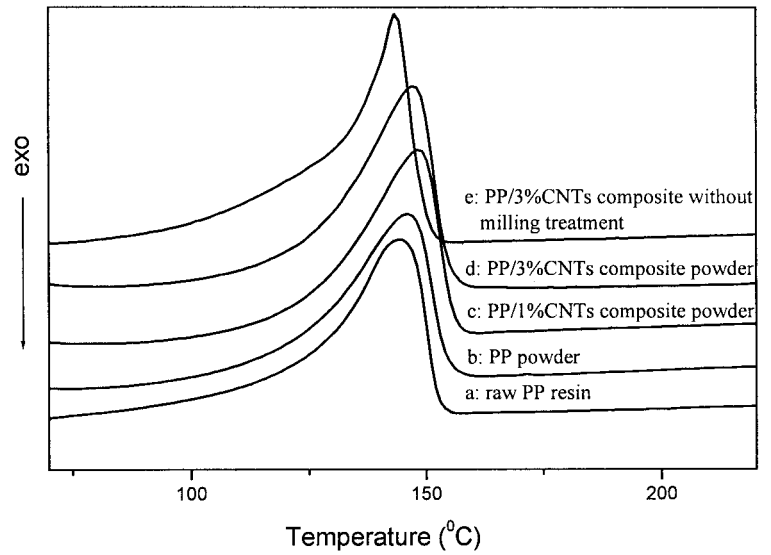

Figure 7 DSC heating thermograms of PP, pan-milled PP/CNT composite powders, and PP/CNT composites without milling treatment.

addition of 1 or 3% CNT, it increased to approximately 148.5 or 147.1°C, respectively. This could be attributed to the fact that the presence of CNTs reduced the mobility and melting entropy of PP.

Effects of CNTs on the crystalline behavior of PP

It is interesting to investigate the effect of CNTs with a high aspect ratio on the crystalline behavior of PP.[31] PP is a semicrystalline polymer. Its main, stable crystal form is the α (monoclinic) form. The orientation of crystallites under stress or in the presence of some fillers with a high aspect ratio, such as magnesium hydroxide or talc, can occur.[32,33] It is believed that the orientation of crystallites can improve the mechanical properties. PP consists predominantly of orientations in the 110, 040, 130, 111, and 041 directions. The 110 and 040 planes are the most important and reveal information about the directions in which the *a* and *b* axes are oriented. The relationship between the orientation of PP in the *a* and *b* axes can be obtained from the ratio of the diffraction intensity of the 110 plane to that of the 040 plane. If the ratio is less than 1.3, the *b* axis lies predominantly to the surface under analysis.

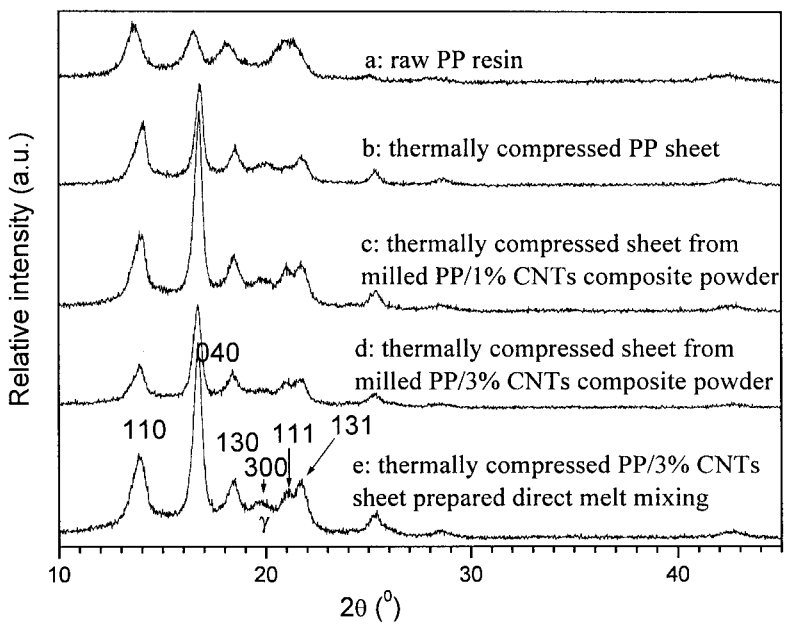

Figure 8 XRD patterns of PP and PP/CNT composite sheets after thermal compression.

TABLE I
I_{110}/I_{040} and XL Calculated from XRD Profiles

	I_{110}/I_{040}	XL (%)
PP4220 resin	1.763	56.8
Compression-molded PP (milled 5 times)	0.943	60.8
Compression-molded PP/1% CNT (milled 20 times)	0.621	64.8
Compression-molded PP/3% CNT (milled 20 times)	0.613	59.1
Compression-molded PP/3% CNT (unmilled)	0.694	59.5

If the ratio is greater than 1.5, then the *a* axis is parallel to the surface. If the ratio lies between these two values, then the mixture of crystallites is isotropic.[34] Figure 8 shows the XRD patterns of PP and PP/CNT composite sheets. Table I summarizes the ratios of the intensity of the 110 plane to the intensity of the 040 plane (I_{110}/I_{040}) and the XL values for the samples. The analysis provided information about the orientation of the continuous PP phase. The I_{110}/I_{040} ratio was 1.76 for the original PP, indicating that the *a* axis was parallel to the surface under analysis. The I_{110}/I_{040} ratio was 0.94 for the molded PP sheets under 10 MPa, indicating that the *b* axis was parallel to the surface. When the content of CNTs was 1 or 3% in the PP matrix, the I_{110}/I_{040} ratio was 0.621 or 0.613, respectively. The decrease in the I_{110}/I_{040} ratio with an increasing amount of CNTs suggests a strong *b*-plane orientation. For the unmilled PP/3% CNT composite, the I_{110}/I_{040} ratio was 0.694, which was higher than that of the milled counterpart. This suggested that the pan milling favored the *b*-plane orientation. Therefore, the presence of the CNTs in the PP matrix highly promoted the orientation in the *b* axis. This should be attributed to the one-dimensional structure of the CNTs and their high aspect ratio.

Figure 9 shows the DSC cooling thermograms of the PP and PP/CNT composite powder. As the concentration of CNTs increased, the crystallization temperature and rate of PP increased. The crystallization temperature (defined as the peak temperature) of the PP resin was 101.7°C. In the presence of 1 or 3% CNT, it increased to 109.1 or 111.0°C, respectively. This suggested that the CNTs acted as nucleating agents for PP. The effect of pan milling on the crystallization behavior was also examined for the PP/3% CNT composite materials obtained from the melt mixing of the corresponding composite powder. The crystallization temperature of the unmilled PP/3% CNT composite material was 108.5°C. In contrast, that of the milled counterpart was 111.0°C. This indicated that there were likely more nucleating sites in the milled PP/3% CNT composite material. The reason is that the number of CNTs after pan milling increased and better dispersion was attained. The XL values calculated from the enthalpy of fusion were 51.5, 52.2, 55.0, 54.1, and 55.9% for the raw PP, PP powder, PP/1% CNT composite powder, PP/3% CNT composite powder, and PP/3% CNT composite without milling, respectively. Apparently, the presence of the CNTs increased the XL values slightly. This is in agreement with the XRD results.

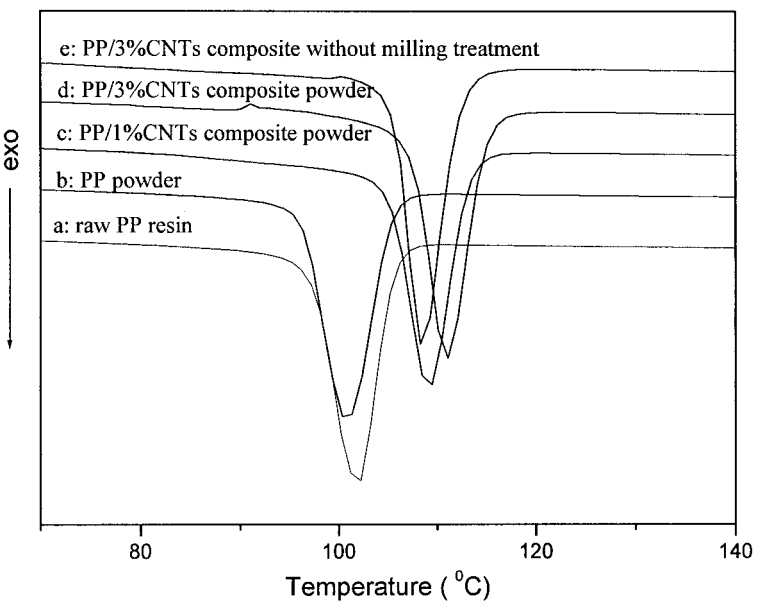

Figure 9 DSC cooling thermograms of PP and PP/CNT composite powders.

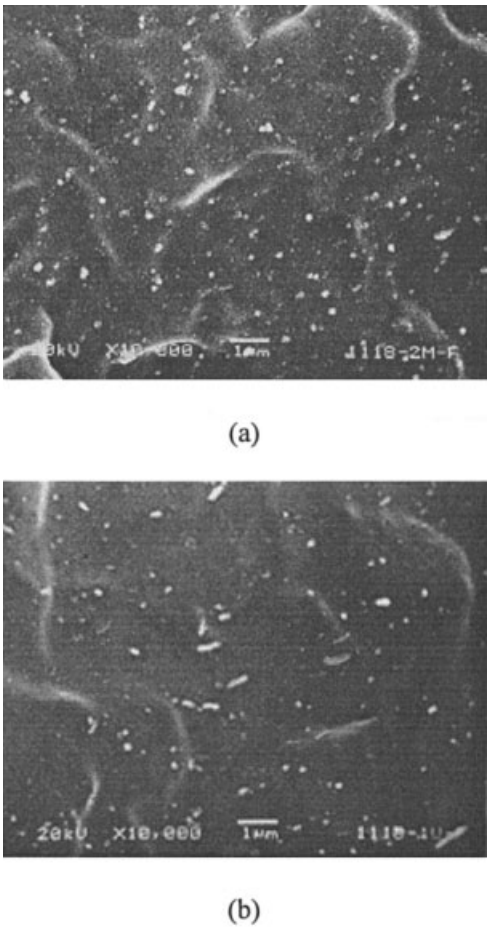

Figure 10 SEM photographs of surfaces, cryogenically fractured in liquid nitrogen, of PP/3% CNT composites (a) with and (b) without mechanochemical milling.

State of the dispersion of the CNTs in PP

Figure 10 shows SEM photographs of cryogenically fractured surfaces in liquid nitrogen for the PP/3% CNT composites. The white-dot regions represent the ends of CNTs that were stretched out off the polymer matrix. For the milled PP/3% CNT composite, the CNTs were uniformly dispersed in PP. This suggested that secondary aggregates and entanglements of the CNTs were broken during the pan milling or during the subsequent melt-mixing process. For the unmilled PP/3% CNT composite, the CNTs were not as well dispersed as those in the milled counterpart. In addition, the CNTs appeared to be longer in the unmilled composite than in the milled one.

Mechanical properties of the PP/CNT composites

Table II lists the tensile properties of the PP and PP/CNT composites. After pan milling, the elongation at break of PP decreased markedly. However, when the CNTs were incorporated, the elongation at break increased. It was as high as 791% for the PP/3% CNT composite. This property increase should be attributed to the changes in the crystal structure and orientation of PP induced by the incorporation of the CNTs. As expected, the presence of the CNTs improved the Young's modulus and yield strength of PP. In comparison with the unmilled PP/3% CNT composite, the milled one had improved mechanical properties. As mentioned previously, a better dispersion of the CNTs, a reduced number of defects, curvatures, and entanglements of the CNTs, and enhanced adhesion between the PP and CNTs all favored improvements in the properties.

CONCLUSIONS

A PP/CNT composite powder was prepared through a solid-state mechanochemical pulverizing process with a laboratory-made pan mill. It was then melt-mixed with a twin-roll masticator to obtain the composite. The process had the following three functions: first, it improved the cohesion between the polymer and CNTs by mechanochemical effects; second, it cut the CNTs and reduced the number of defects and entanglements of long CNTs; and third, it improved the dispersion of the CNTs in PP. SEM showed that after 20 milling cycles, the average particle size of a PP/3% CNT composite powder was as small as a few micrometers. Its corresponding surface area measured by BET increased to 4.29 m^2/g. During pan milling, the original CNTs, a few micrometers long, were cut to 0.4–0.5 μm and became straighter and more uniform. The addition of the CNTs increased the crystallization rate and crystalliza-

TABLE II
Mechanical Properties of PP and PP/CNT Composites

	Tensile strength (MPa)	Yield strength (MPa)	Young's modulus (MPa)	Strain at break (%)
PP	33	21	837	716
PP, milled 5 times	27	27	995	151
PP/CNT (1%), milled 20 times	33	25	1140	764
PP/CNT (3%), milled 20 times	33	27	926	791
PP/CNT (3%), unmilled	28	24	911	716

tion temperature of PP and reduced its XL value. It induced a strong *b*-plane orientation. The Young's modulus and yield strength of PP also increased.

References

1. Shaffer, M. S. P.; Windle, A. H. Adv Mater 1999, 11, 937.
2. Kashiwagi, T.; Grulke, E.; Hilding, J.; Harris, R.; Awad, W.; Douglas, J. Macromol Rapid Commun 2002, 23, 761.
3. Thostenson, E. T.; Ren, Z. F.; Chou, T. W. Compos Sci Technol 2001, 61, 1899.
4. Kearns, J. C.; Robert, L. J Appl Polym Sci 2002, 86, 2079.
5. Andrews, R.; Jacques, D.; Minot, M.; Rantell, T. Macromol Mater Eng 2002, 7, 395.
6. Safadi, B.; Andrews, R.; Grulke, E. A. J Appl Polym Sci 2002, 84, 2660.
7. Ajayan, P. M.; Stephan, O.; Colliex, C.; Tranth, D. Science 1994, 265, 1212.
8. Calvert, P. Nature 1999, 399, 210.
9. Geng, H. Z.; Rosen, R.; Zheng, B.; Shimoda, H.; Fleming, L.; Liu, J.; Zhou, O. Adv Mater 2002 14, 1387.
10. Gong, X.; Liu, J.; Baskran, S.; Voise, R. D.; Young, J. S. Chem Mater 2000, 12, 1049.
11. Frankland, S. J. V.; Caglar, A.; Brenner, D. W.; Griebel, M. J Phys Chem B 2002, 106, 3873.
12. Gojny, F. H.; Nastalczyk, J.; Roslaniec, Z.; Schulte, K. Chem Phys Lett 2003, 370, 820.
13. Lin, Y.; Rao, A. M.; Sadanadan, B.; Kenik, E. A.; Sun, Y. P. J Phys Chem B 2002, 106, 1294.
14. Mitchell, C. A.; Bahr, J. L.; Arepalli, S.; Tour, J. M.; Krishnamoorti, R. Macromolecules 2002, 35, 8825.
15. Koshio, A.; Yudasaka, M.; Zhang, M.; Iijima, S. Nano Lett 2001, 1, 361.
16. O'Connell, M. J.; Boul, P.; Ericson, L. M.; Huffman, C.; Wang, Y. Chem Phys Lett 2001, 342, 265.
17. Tang, B. Z.; Xu, X. Macromolecules 1999, 32, 2569.
18. Mccormick, P. G.; Tsuzuki, T.; Robinson, J. S.; Ding, J. Adv Mater 2001, 13, 1008.
19. Frost, R. L.; Mako, E.; Kristof, J.; Horvath, E.; Kloprogge, J. T. Langmuir 2001, 17, 4731.
20. Xu, X.; Guo, S. Y.; Wang, Z. Q. J Appl Polym Sci 1997, 64, 2273.
21. Chen, Z.; Liu, C. S.; Wang, Q. Polym Eng Sci 2001, 41, 1187.
22. Wang, Q.; Cao, J. Z.; Huang, J.; Xu, X. Polym Eng Sci 1997, 37, 1091.
23. Liu, C. S.; Wang, Q. J Appl Polym Sci 2000, 78, 2191.
24. Yin, J. H.; Mo, Z. S. Modern Polymer Physics; Press of Science: Beijing, China, 2002; Chapter 16, p 473.
25. Fatou, J. G. Eur Polym J 1971, 7, 1057.
26. Roy, S. K.; Kyu, T.; Manley, R. S. J. Macromolecules 1998, 21, 499.
27. Chen, J.; Hamon, M. A.; Hu, H.; Chen, Y. S.; Rao, A. M.; Eklund, P. C.; Haddon, R. C. Science 1998, 282, 95.
28. Kim, Y. A.; Hayashi, T.; Fukai, Y.; Endo, M.; Yanagisawa, T.; Dresselhaus, M. S. Chem Phys Lett 2002, 355, 279.
29. Pierard, N.; Fonseca, A.; Konya, Z.; Willems, I.; Tendeloo, G. V.; Nagy, J. B. Chem Phys Lett 2001, 335, 1.
30. Biro, L. P. Carbon Filaments and Nanotubes: Common Origins, Differing Applications; Kluwer: Norwell, MA, 2001; p 187.
31. Bhattacharyya, A. R.; Creekumar, T. V.; Liu, T.; Kumar, S.; Ericson, L. M.; Hauge, R. H.; Smalley, R. E. Polymer 2003, 44, 2373.
32. Cook, M.; Harper, J. F. Adv Polym Technol 1998, 17, 53.
33. Fujiyama, M.; Wakino, T. J Appl Polym Sci 1991, 42, 9.
34. Rybnikar, F. J Appl Polym Sci 1989, 38, 1479.